

# QCD Dynamics and Hadron Production in High-Energy Nuclear Collisions at LHCb

---

**Saliha Bashir**<sup>a,\*</sup>

<sup>a</sup>*Faculty of Physics and Applied Computer Science, AGH University of Krakow,  
Al. Mickiewicza 30, 30-059 Krakow, Poland*

*E-mail:* [bashir@agh.edu.pl](mailto:bashir@agh.edu.pl)

This study investigates dijet and neutral pion production in high-energy nuclear collisions in the LHCb detector. The obtained measurements offer crucial insights into Quantum Chromodynamics (QCD), understanding of parton distribution functions, nuclear structure, and particle production dynamics. Specifically, the nuclear modification factor for neutral pions in proton-lead collisions at 8.16 TeV reveal notable first evidence enhancement in the backward region providing constraints on models of nuclear structure. Furthermore, the inclusive  $b\bar{b}$  and  $c\bar{c}$ -dijet production cross-sections in the forward region of pp collisions at 13 TeV align with next-to-leading order theoretical predictions. These findings on dijet and neutral pion production offer complementary perspectives on PDFs and nuclear structure, crucial for comprehending QCD dynamics in high-energy nuclear collisions and refining theoretical models.

*The European Physical Society Conference on High Energy Physics (EPS-HEP2023),  
21-25 August 2023  
Hamburg, Germany*

---

\*Speaker

## 1. QCD physics at LHCb experiment

The LHCb experiment [1] is the forward spectrometer designed for the particles containing  $b$ - or  $c$ - quarks. It covers a unique phase space  $2.0 < \eta < 5.0$ , complimentary to other experiments. LHCb has an excellent vertex reconstruction system, which allows to tag jets by reconstructing secondary vertices formed by tracks inside the jet. Precision measurements of jet production and fragmentation are important tests of perturbative QCD and hadronization models. In this way it possible to study the parton distribution functions (PDFs) and proton structure at high  $x$  values and at low  $x$  values and high  $Q^2$ , where  $x$  is the longitudinal momentum fraction of proton carried by the parton and  $Q^2$  is the energy scale of interaction. On the other hand, the production of neutral pions is sensitive to cold nuclear matter (CNM) effects, these effects in the collinear factorization framework are encoded into nuclear parton distribution functions (NPDFs) and the parton-parton collision dynamics are described by perturbative quantum chromodynamics (pQCD). These NPDFs are determined using fits to data and are poorly constrained for partons with momentum fraction  $x$  smaller than about  $10^{-4}$ . Measurement of neutral pions with the LHCb detector can provide constraints on NPDFs in the identification of parton saturation effects. These effects are visible on the lower values of  $x$ .

## 2. $b\bar{b}$ and $c\bar{c}$ differential cross-sections

Measurements of  $b\bar{b}$  and  $c\bar{c}$  hadrons provide an excellent test of pQCD in the forward region. As  $b\bar{b}$ - and  $c\bar{c}$ -dijet differential cross-sections can be calculated as a function of dijet kinematics, comparisons between data and predictions provide critical test of next-to-leading order (NLO) pQCD calculations. Measurements of differential cross-sections of heavy flavor dijets can also be a sensitive probe of the parton distribution functions (PDFs) of the proton. This paper uses the 2016 data sample collected with integrated luminosity of  $1.6 \text{ fb}^{-1}$ . After the calculation of cross-sections the ratio of the  $c\bar{c}$  to  $b\bar{b}$  is also determined. Differential cross-section measurements have been performed with respect to four kinematic variables: leading jet  $p_T$ , leading jet  $\eta$ , dijet invariant mass  $m_{jj}$  and difference in jet rapidity  $\Delta y^* = 1/2|y_0 - y_1|$ . The jets are reconstructed using particle flow objects as input. The objects are combined employing the anti- $k_T$  algorithm. To distinguish the flavors a heavy-flavor jet-tagging algorithm referred as "SV-tagging", which reconstructs secondary vertices (SV) was used which using tracks inside and outside of jet. To further distinguish the light-flavor jets from heavy-flavor jets and b-jets from c-jets two multi variate analysis (MVA) methods to get flavor composition, based on Boosted Decision Trees, were used to get the jet flavor composition. Four tagging observables are used for disentangling the  $b\bar{b}$  and  $c\bar{c}$  processes from the background: the output of the classifiers  $\text{BDT}_{bc|q}$  and  $\text{BDT}_{b|c}$  for the leading jet and  $\text{BDT}_{bc|q}$  and  $\text{BDT}_{b|c}$  for the second jet. In principle a four-dimensional fit would give the best result in terms of the statistical uncertainty, but this is not optimal given the finite simulated sample sizes. Instead, two new observable are built, introducing linear combinations of the four tagging observable. These observable are called  $t_0$  for the light/heavy (udsg/bc) separation and  $t_1$  for the b/c separation. The result of this fit is shown in figure 1.

The yields in each of the bins of the observables are used to calculate the differential cross-sections at the generator level, using an unfolding technique to correct for bin migrations due to

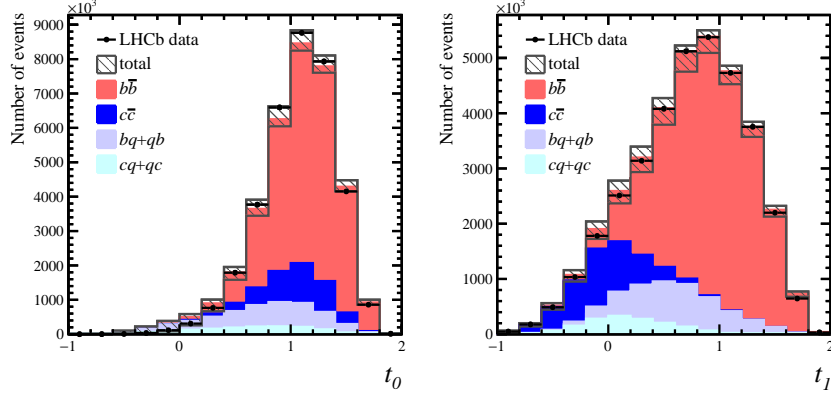


**Figure 1:** Result of the fit to the observable  $(t_0, t_1)$ , that are obtained with multivariate classifiers trained for the separation of b, c and light jets [2].

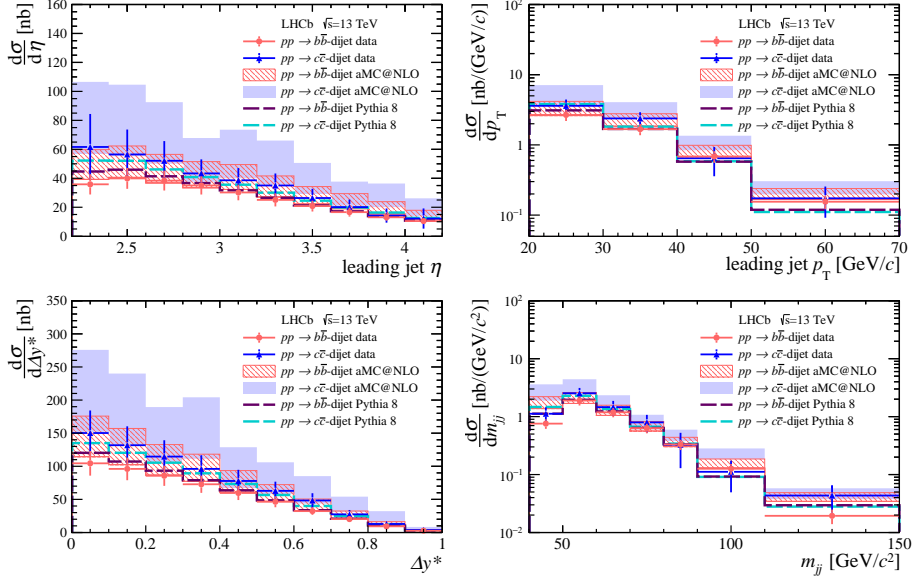


**Figure 2:** Differential  $b\bar{b}$  and  $c\bar{c}$ -dijet cross-sections as a function of the (top left) leading jet  $\eta$ , (top right) the leading jet  $p_T$ , (bottom left)  $\Delta y^*$  and (bottom right)  $m_{jj}$ . The error bars represent the total uncertainties. The NLO predictions obtained with Madgraph5 aMC@NLO + Pythia are shown [2].

detector effects and resolution. The differential cross-section is calculated as a function of leading jet  $p_T$ , leading jet  $\eta$ ,  $\Delta y^*$  and  $m_{jj}$  and is shown in figure 2. The total measured  $b\bar{b}$ -dijet cross-section in fiducial region is:

$$\sigma(pp \rightarrow b\bar{b} - dijetX) = 53.0 \pm 9.5 \pm 2.1 \text{ nb} \quad (1)$$

and for  $c\bar{c}$ -dijet cross-section in the fiducial region is:

$$\sigma(pp \rightarrow c\bar{c} - dijetX) = 72.6 \pm 16.1 \pm 2.9 \text{ nb} \quad (2)$$

where the first uncertainty is the combined statistical and systematic uncertainty and the second is due to the precision of the luminosity calibration. Finally, the ratio of the ratio of the  $b\bar{b}$  and  $c\bar{c}$

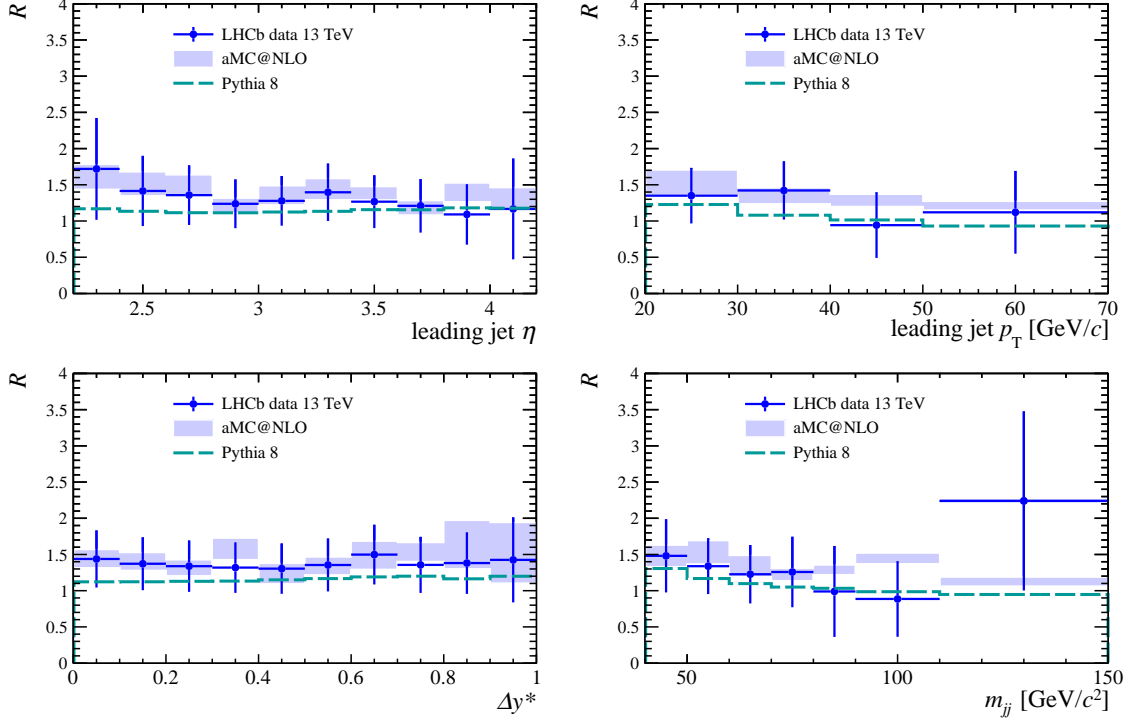


**Figure 3:** Measured  $b\bar{b}$  and  $c\bar{c}$ -dijet cross-section ratio as a function of the (top left) leading jet  $\eta$ , (top right) the leading jet  $p_T$ , (bottom left)  $\Delta y^*$  and (bottom right)  $m_{jj}$ . The error bars represent the total uncertainties. The NLO predictions obtained with Madgraph5 aMC@NLO + Pythia are shown [2].

cross-section as a function of the same kinematic variables were calculated and are presented in figure 3.

The measured ratio between the two cross-sections is:

$$R = \frac{\sigma(pp \rightarrow c\bar{c} - dijetX)}{\sigma(pp \rightarrow b\bar{b} - dijetX)} = 1.37 \pm 0.27 \quad (3)$$

The total cross-section and ratio between the two are compatible with the Madgraph5 aMC@NLO + Pythia expectation within the total uncertainties. This is the first  $c\bar{c}$ -dijet differential cross-section measurement at a hadron collider.

### 3. Nuclear Modification factor of neutral pions

Neutral pion production is an important probe of nuclear effects in heavy ion collisions.  $\pi^0$  production is particularly sensitive to cold nuclear matter (CNM) effects and is described in the  $pPb$  collisions using the collinear factorization framework where CNM effects are encoded into nuclear parton distribution functions (NPDFs). The parton-parton collision dynamics are described by perturbative quantum chromodynamics (pQCD). At low  $x$  and low momentum transfer  $Q$ , the parton number density may become so large that the parton saturation effects become sizable. The nuclear modification factor of neutral pions is defined as:

$$R_{pPb} = \frac{1}{A} \frac{d\sigma_{pPb}/dp_T}{d\sigma_{pp}/dp_T}, \quad (4)$$

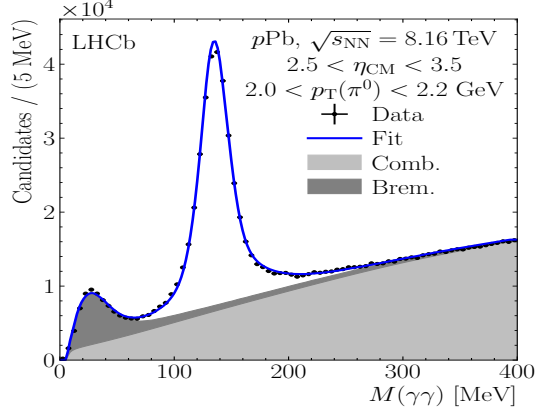


**Figure 4:** Invariant mass distribution in forward p-Pb collisions in a particular bin of  $p_T$  and  $\eta$ . Fit results are overlaid with the total fit shown as a solid line. The combinatorial (Comb) and bremsstrahlung (Brem) backgrounds are shown as light and dark shaded regions, respectively [3].

where,  $A = 208$  represents atomic mass number of the lead nucleus. The quantities  $d\sigma_{pp}$  and  $d\sigma_{pPb}$  correspond to the differential production cross-sections of  $\pi^0$  in  $pPb$  and  $pp$  collisions, respectively. It is determined using data from  $pPb$  collisions at  $\sqrt{s} = 8.16$  TeV, which includes limited sample of unbiased  $pp$  collisions collected with the LHCb detector. Also, for reference, a cross-section for  $pp$  collisions is established by interpolating between measurements conducted in  $pp$  collisions at 5 and 13 TeV. Neutral pions are reconstructed using their decays to pair of photons, reconstructed directly in electromagnetic calorimeter or as an electron-positron pair in the detector material. An example of  $\pi^0$  candidate invariant mass [ $M(\gamma\gamma)$ ] distribution in one interval of  $p_T$  and  $\eta$  is shown in figure 4.

The corrected  $\pi^0$  distribution is shown in figure 5. The nuclear modification factor (NDF) shows a Cronin like enhancement at the backward pseudorapidity and a strong suppression at forward pseudorapidity. The measurements are compared to next-to-leading order PQCD calculations. The measurement uncertainties in the forward region are much smaller than the NDF uncertainties, indicating that this measurement can provide powerful constraints on NPDFs at low  $x$ . The enhancement in the backward region, specifically between 2 and 4 GeV is larger than expected by the PQCD calculations suggesting that effects not described by NPDFs contribute to enhancement.

#### 4. Conclusion

The LHCb experiment serves as a versatile forward detector with a broad range of capabilities. This report highlights the most recent findings in QCD physics measurements conducted at LHCb. The first analysis was related to the differential cross-section of jets which provide an excellent test of the pQCD in the forward region. And the second analysis is the study of neutral pions which play an important role in the study of CNM effects. These studies provide an additional angle to examine PDFs and nuclear structure. These aspects are essential in gaining a comprehensive understanding of QCD dynamics in high-energy nuclear collisions and in refining theoretical frameworks.

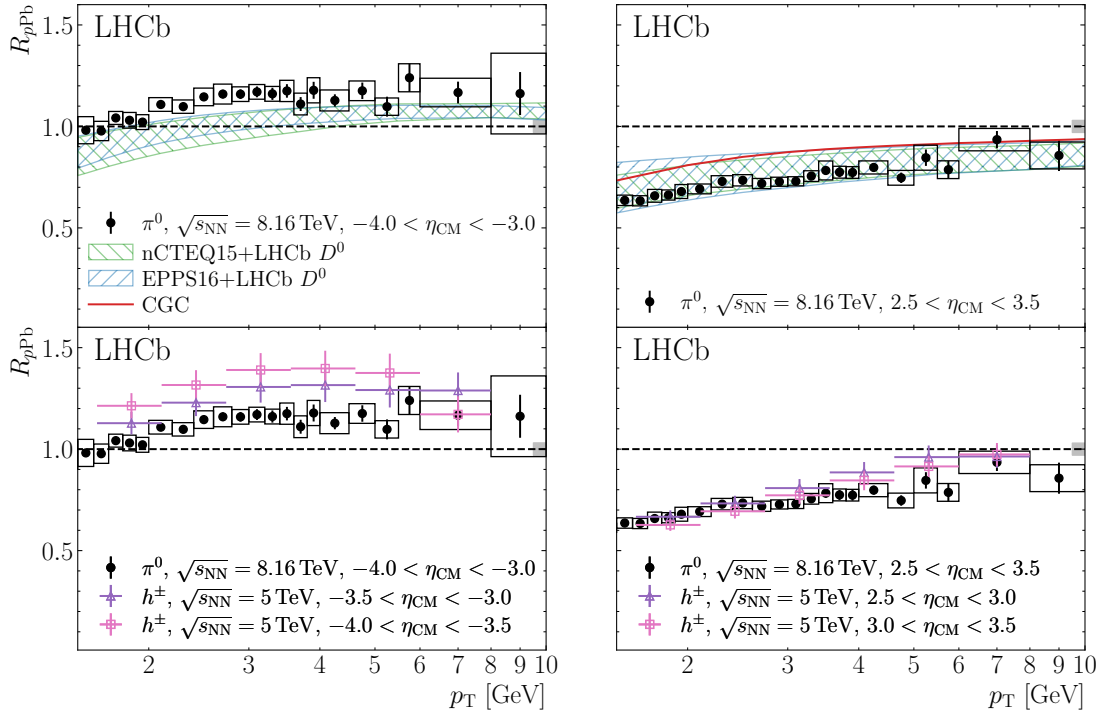


**Figure 5:** Measured  $\pi^0$  nuclear modification factor in the (left) backward and (right) forward  $\eta$  regions. Error bars show the statistical uncertainty, while the open boxes show the  $p_T$ -dependent systematic uncertainties. The solid gray boxes show the overall normalization uncertainties from the luminosity estimate and efficiency correction factors. The results are compared to (top) theoretical predictions and (bottom) to charged-particle data. The hatched regions show the NPDF uncertainties of the PQCD calculations. The vertical error bars on the charged-particle results show the combined systematic and statistical uncertainties [3].

## References

- [1] A. Augusto Alves, Jr. et al. The LHCb Detector at the LHC. *JINST*, 3:S08005, 2008. doi: [10.1088/1748-0221/3/08/S08005](https://doi.org/10.1088/1748-0221/3/08/S08005).
- [2] Roel Aaij et al. Measurement of differential  $b\bar{b}$ - and  $c\bar{c}$ -dijet cross-sections in the forward region of  $pp$  collisions at  $\sqrt{s} = 13$  TeV. *JHEP*, 02:023, 2021. arXiv:2010.09437, doi: [10.1007/JHEP02\(2021\)023](https://doi.org/10.1007/JHEP02(2021)023).
- [3] Aaij and et al. Nuclear modification factor of neutral pions in the forward and backward regions in  $p$ -Pb collisions. *Phys. Rev. Lett.*, 131:042302, Jul 2023. URL: <https://link.aps.org/doi/10.1103/PhysRevLett.131.042302>, doi: [10.1103/PhysRevLett.131.042302](https://doi.org/10.1103/PhysRevLett.131.042302).

## Acknowledgement

This work was partially supported by the National Research Centre, Poland (NCN), grants No.UMO-2019/35/O/ST2/00546 and by Polish Ministry of Science and Higher Education MNiSW.